

Heavy Majorana neutrinos in e^-e^- collisions ¹

Christoph Greub

Deutsches Elektronen-Synchrotron DESY, Hamburg

Peter Minkowski

*Institute for Theoretical Physics, University of Bern,
Sidlerstr. 5, CH-3012 Bern, Switzerland*

Abstract

We discuss the process $e^-e^- \rightarrow W^-W^-$ mediated by heavy Majorana neutrino exchange in the t - and u channel. In our model the cross section for this reaction is a function of the masses (m_N) of the heavy Majorana neutrinos and mixing parameters (U_{eN}) originating from mixing between the ordinary left-handed standard model neutrinos and additional singlet right-handed neutrino fields. Taking into account the standard model background and constraints from low energy measurements, we present discovery limits in the (m_N, U_{eN}^2) plane. We also discuss how to measure in principle the CP violating phases, i.e., the relative phases between the mixing parameters.

(To be published in the Proceedings of the 1996 DPF/DPB Summer Study
on New Directions for High Energy Physics (Snowmass 96).)

¹Work supported in part by Schweizerischer Nationalfonds

1 Introduction

The question why the masses of the observed neutrinos are much lighter than those of the charged leptons is a central unsolved problem in particle physics. An attractive scenarios to understand this is the following: Adding right-handed singlet neutrino fields to the standard model, the resulting mass spectrum can be such that there are 3 essentially zero mass Majorana neutrinos and additional heavy Majorana neutrinos. While in the generic case the masses of these heavy neutrinos are too large to detect observable consequences at present and future colliders, it not excluded however, that their masses are in the range of a few TeV and that their coupling strength to the charged leptons are rather large. For the latter case, the phenomenology for e^+e^- collisions where heavy Majorana neutrinos can be directly produced via t - channel W and s - channel Z^0 exchange, has been worked out in detail in [1]. The main conclusion is that the cross sections and designed luminosities are large enough to find heavy Majorana neutrinos essentially up to the kinematical limit, i.e., up to $m_N \approx \sqrt{s}$, provided that the relevant mixing angles are near the present bounds inferred from low energy data. A similar conclusion also holds for single Majorana neutrino production in $e\gamma$ collisions. Another attractive reaction to be discussed in detail in this paper is $e^-e^- \rightarrow W^-W^-$, which is mediated by t - and u - channel Majorana neutrino exchange (see Fig. 1). As the neutrinos do not have to be produced in this reaction, one is potentially sensitive to neutrino masses which exceed \sqrt{s} . Therefore, the aim of this paper is to work out the discovery region for such neutrinos in the parameter space (masses and mixing angles), taking into account standard model background reactions.

In the second part of this introduction we present the model and list the present bounds on masses and mixing angles inferred from low energy precision measurements. In section II we discuss the signal reaction $e^-e^- \rightarrow W^-W^-$, while section III deals with the simulation of the standard model background. In section IV we present the discovery limits in the (m_N, U_{eN}^2) plane. Section V finally deals with the question of how one can measure in principle the relative phases of the mixing angles; the presence of such phases is a necessary condition to observe CP violation in reactions like $e^-e^- \rightarrow W^-W^-$.

1.1 The Model

As in the standard model (SM) only left-handed neutrino fields are present, a Dirac mass (m_D) term for the neutrinos cannot be written down; also a Majorana mass term (m_M) involving only the left-handed neutrino fields (ν_L) cannot be constructed consistently within the SM because this would require Higgs-Triplets which are absent in the SM. Consequently, neutrinos are exactly massless in the SM. There are, however, many extensions of the SM (like $SO(10)$, E_6 , ...) with k extra neutrino fields (ν_R) which are singlets under the SM gauge group G_{SM} . In a generic case symmetry breaking then induces the mass term

$$L_\nu^{mass} = -\overline{\nu_L} m_D \nu_R - \frac{1}{2} \overline{\nu_R^c} m_M \nu_R + h.c. \quad , \quad (1)$$

where m_D is a $(3 \times k)$ Dirac mass matrix and m_M is a $(k \times k)$ Majorana mass matrix. As an example, the grand unified group $SO(10)$ can break to the SM group through the chain

$$SO(10) \xrightarrow{\Lambda_{GUT}} G_{SM} \times U(1)_{B-L} \xrightarrow{v'} G_{SM} \xrightarrow{v} SU(3)_c \times U(1)_{em} \quad , \quad (2)$$

where Λ_{GUT} , v' and $v = 174$ GeV are the respective breaking scales in this chain. In this example, the Dirac- and Majorana mass matrices are of the form

$$m_D = g \cdot v \quad , \quad m_M = h \cdot v' \quad , \quad (3)$$

where g and h are matrices of Yukawa couplings. It is conceivable that the residual $B - L$ breaking scale v' is as low as a few TeV ; in this case also the Majorana mass term is expected to be relatively light.

To get the mass eigenstates, one has to diagonalize the neutrino mass matrix by means of a unitary $(3 + k \times 3 + k)$ matrix U . The resulting mass eigenstates are 3 light Majorana neutrinos ν_i with masses m_{ν_i} and k heavy Majorana neutrinos N_i with masses m_{N_i} . Expressing the weak eigenstates in the charged current by the corresponding mass eigenstates², we get the $W - e - N$ ($W - e - \nu$) vertices relevant for our process $e^-e^- \rightarrow W^-W^-$:

$$L_{W_{e\nu}, W_{eN}} = \frac{g}{\sqrt{2}} \left(\sum_{\nu} \bar{e} \gamma_{\mu} L U_{e\nu} \nu + \sum_N \bar{e} \gamma_{\mu} L U_{eN} N \right) W^{\mu} \quad . \quad (4)$$

It is instructive to look for a moment at the simpler $1 + 1$ dimensional case with only one left-handed and one right-handed neutrino field. The masses and the mixing angle U_{eN} are given by the see-saw formulae [2]

$$m_{\nu} \approx \frac{m_D^2}{m_M} \quad , \quad m_N \approx m_M \quad , \quad U_{eN} \approx \frac{m_D}{m_M} \quad . \quad (5)$$

In this case, the bounds on the light neutrinos imply that the mixing angle U_{eN} has to be very small; consequently the cross section in $e^-e^- \rightarrow W^-W^-$ is much too small to be observed. In the general $3 + k$ dimensional case, however, it is possible, that the 3 light neutrinos are exactly massless while the mixing angles U_{eN} remain finite (i.e. nonzero)! This means that there is some chance to find heavy neutrinos with rather large cross sections through the process $e^-e^- \rightarrow W^-W^-$.

In the following, we assume the light neutrinos to be massless (minimal mass generating case) and the mixing angles U_{eN} and heavy masses m_N to be essentially free parameters.

1.2 Constraints on masses and mixing angles

Before listing the constraints from low energy measurements, we would like to point out a model constraint. Assuming that there are no Higgs triplet fields, the Majorana mass term for the left-handed neutrinos is absent (as in eq. (1)). This implies the relation

$$\sum_{\nu} m_{\nu} U_{e\nu}^2 + \sum_N m_N U_{eN}^2 = 0 \quad , \quad (6)$$

or in the minimal mass generating case ($m_{\nu} = 0$)

$$\sum_N m_N U_{eN}^2 = 0 \quad . \quad (7)$$

We now list the experimental constraints:

²We assume without loss of generality that the mass matrix of the charged leptons has been diagonalized prior to the neutrino mass matrix.

- Charged current universality implies that $|U_{eN}|^2 < 4 \times 10^{-3}$. The LEP-1 data lead to similar bounds [3].
- Heavy Majorana neutrinos mediate the rare decay $\mu \rightarrow e\gamma$. Non-observation of this decay leads to the strong bound $|\sum_N U_{\mu N} U_{eN}^*| < 2 \times 10^{-4}$. This bound, however, does not necessarily lead to a more stringent bound on U_{eN} than charged current universality.
- The non-observation of neutrinoless double beta decay $\beta\beta_{0\nu}$ implies a bound on both, the light and heavy neutrino sector. The best present evidence on the non-observation of the $\beta\beta_{0\nu}$ reaction is from the experimental limit on the process ${}^{76}\text{Ge} \rightarrow {}^{76}\text{Se} e^- e^-$, with $\tau_{1/2} > 5 \times 10^{24}$ years. For light neutrinos the bound reads

$$\left| \sum_{\nu} U_{e\nu}^2 m_{\nu} \right| \leq \text{few eV} \quad . \quad (8)$$

In the minimal mass generating case ($m_{\nu} = 0$) this bound is satisfied automatically. For heavy Majorana neutrinos the bound is of the form

$$\left| \sum_N \frac{U_{eN}^2}{m_N} \right|^2 \times |\text{hadr. matrix element}|^2 \leq \frac{1}{\tau_{1/2}} \quad . \quad (9)$$

A recent paper [4] shows that in the older literature the hadronic matrix elements have been strongly overestimated. Taking the new estimates for the hadronic matrix elements, the bound becomes

$$\left| \sum_N \frac{U_{eN}^2}{m_N} \right| < 6 \times 10^{-3} \text{ TeV}^{-1} \quad . \quad (10)$$

2 Signal

In the minimal mass generating case, where the light neutrinos are exactly massless by definition, only the heavy Majorana neutrinos (N_i) contribute to the process $e_L^- e_L^- \rightarrow W^- W^-$. The corresponding Feynman diagrams are shown in Fig. 1. For $\sqrt{s} \gg m_W$ the cross section is to-

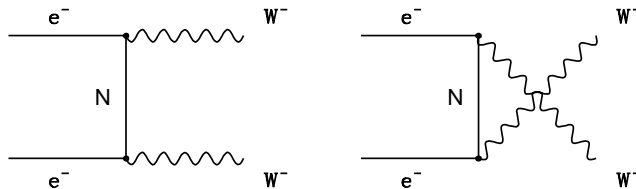


Figure 1: Feynman diagrams for the process $e_L^- e_L^- \rightarrow W^- W^-$.

tally dominated by the production of longitudinally polarized W^- . To leading order in m_W/\sqrt{s} and in tree approximation the angular distribution $d\sigma(e_L^- e_L^- \rightarrow W^- W^-)/d\cos\theta$ is given by the expression [5]

$$\frac{d\sigma}{d\cos\theta} = \frac{G_F^2}{8\pi} \left| \sum_N m_N U_{eN}^2 \left(\frac{t}{t - m_N^2} + \frac{u}{u - m_N^2} \right) \right|^2 \quad , \quad (11)$$

with $t = -(s/2)(1 - \cos \theta)$ and $u = -(s/2)(1 + \cos \theta)$. The general relation between mass and mixing parameters given in eq. (6) for all neutrino flavors ensures unitarity and renormalizability. As a consequence of eq. (7) [or eq. (6)], the cross section in eq. (11) vanishes in the limit $\sqrt{s} \rightarrow \infty$ because the leading constant term becomes proportional to $\sum_N m_N U_{eN}^2$. Another feature which is easily seen from eqs. (11) and (7) is that the heavy Majorana neutrinos have to be degenerate in mass in order to have a non-zero cross section.

Note, that in the limit where the masses of all heavy Majorana neutrinos are much larger than \sqrt{s} , formula (11) could be further approximated to read

$$\frac{d\sigma}{d\cos\theta} = \frac{G_F^2}{8\pi} \left| \sum_N \frac{U_{eN}^2}{m_N} \right|^2 s^2 \quad , \quad m_W \ll \sqrt{s} \ll m_N \quad . \quad (12)$$

In the subsequent numerical analysis the lightest of the heavy neutrino masses is singled out for simplicity in the scenario

$$m_W \ll \sqrt{s} \leq m_{N_1} \ll m_{N_2}, m_{N_3}, \dots \quad . \quad (13)$$

The results are then parametrized by the mass $m_N (= m_{N_1})$ and the corresponding mixing angle U_{eN} .

In the reaction $e_L^- e_L^- \rightarrow W^- W^-$ the invariant mass of the $W^- W^-$ pair equals \sqrt{s} ; this is in contrast to all the background reactions we discuss later, where the invariant mass of the $W^- W^-$ pair reaches \sqrt{s} only in very special kinematical configurations. Therefore, this invariant mass is an essential variable to get rid of the background. To fully exploit this, we concentrate on the hadronic decay modes of the $W^- W^-$ boson pair where all the decay products can be detected (no neutrinos as in the purely leptonic or semileptonic decay mode). The branching ratio of the $W^- W^-$ pair into the three possible channels is given roughly by

$$\begin{aligned} BR(W^- W^- : \text{both } W \text{ decay hadronically}) &= \frac{36}{81} \\ BR(W^- W^- : \text{both } W \text{ decay leptonically}) &= \frac{9}{81} \\ BR(W^- W^- : \text{one decays hadr., the other lept.}) &= \frac{36}{81} \end{aligned}$$

Before discussing the background it is instructive to see that the number of signal events (using eqs. (11) and (14)) can be rather large: For $\sqrt{s} = 500$ GeV, $m_N = 1$ TeV and $U_{eN}^2 = 4 \times 10^{-3}$ the production cross section for $W^- W^-$ followed by hadronic decay of both W^- is $\sigma = 1.2$ fb; this corresponds to 60 events assuming a luminosity of $L = 50$ fb $^{-1}$.

3 Background

The most important backgrounds come from the reactions $e^- e^- \rightarrow W^- W^- \nu \nu$ (1), $e^- e^- \rightarrow W^- Z^0 \nu e^-$ (2), $e^- e^- \rightarrow Z^0 Z^0 e^- e^-$ (3), and $e^- e^- \rightarrow W^- W^+ e^- e^-$ (4), where the gauge bosons decay hadronically and the charged leptons escape along the beam pipe. If the jet charges could be reconstructed, then of course only reaction (1) would remain as a background. In this study we assume that this is not possible, hence deriving rather conservative discovery limits. While (1), (2) and (3) have been calculated by Cuypers et al. [8], the process (4) has been included

by Barger et al. [9]. As mentioned earlier, the invariant mass of the two vector bosons is in general much smaller than \sqrt{s} , because of the additional leptons in the final state (see also Fig. 3). However, there is a tail in the invariant mass distributions of the gauge boson pairs in the background reactions extending up to \sqrt{s} , because the additional leptons are essentially massless. Given the fact that the cross section of the background reaction (4) is more than two orders of magnitude larger than the signal (using optimistic parameters for m_N and U_{eN}) one should try to further reduce the background by imposing additional suitable cuts which do not affect the signal significantly. To do such studies, we wrote a Montecarlo simulation [11] of the signal and the background. Reaction (4) is clearly the most serious background source, because first, it has by far the largest cross section [9] and second, this cross section is dominated by configurations where the final state electrons disappear in the beampipe. We therefore only take into account this background reaction. We calculated reaction (4) in the Weizsäcker-Williams approximation for left-handed electron beams, which means that we have to work out in a first step the cross sections for the subprocess $\gamma\gamma \rightarrow W^+W^- \rightarrow jets$ for polarized on-shell photons. By calculating directly the matrix elements with 4 fermions in the final state and then doing the narrow width approximation of the W -propagators we have correctly incorporated the polarization effects of the intermediate vector bosons. In a second step we convolute the $\gamma\gamma$ cross sections with the appropriate Weizsäcker-Williams photon distribution functions. The corresponding three Feynman diagrams are shown in Fig. 2. As a check, we compared our

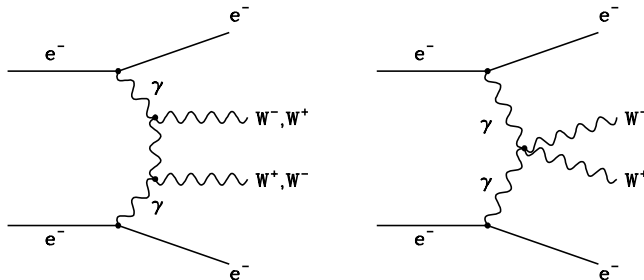


Figure 2: Feynman diagrams for the background process $e_L^- e_L^- \rightarrow W^+W^- e^- e^-$. Only those three diagrams are shown which contribute in the Weizsäcker-Williams approximation.

Weizsäcker-Williams results for $e^- e^- \rightarrow W^- W^+ e^- e^-$ with the exact results in ref. [9] and found good agreement. The resulting invariant mass distribution of the final state hadrons is shown in Fig. 3. Needless to say, this reaction is only a background, if the final state electrons disappear in the beam direction. However, as seen in Fig. 4 of ref. [10] in these proceedings, this background can only be reduced by a few percent when imposing a realistic angular cut on the electron directions.

In order to reduce the background we require the hadronic mass m_{had} to be larger than a certain critical value m_{had}^{crit} . For each \sqrt{s} we do the analysis for the two typical values $m_{had}^{crit} = 0.90 \times \sqrt{s}$ and $m_{had}^{crit} = 0.80 \times \sqrt{s}$, respectively. Figs. 4 and 5 illustrate that the typical average transverse momentum $p_\perp(aver.)$ of the four jets, defined as $p_\perp(aver.) = (1/4) [|p_\perp|(1) + \dots + |p_\perp|(4)]$ is higher for the signal than for the background (after imposing the m_{had}^{crit} -cut).

One therefore can further enhance the signal/background ratio by imposing a lower cut on the variable $p_\perp(aver.)$.

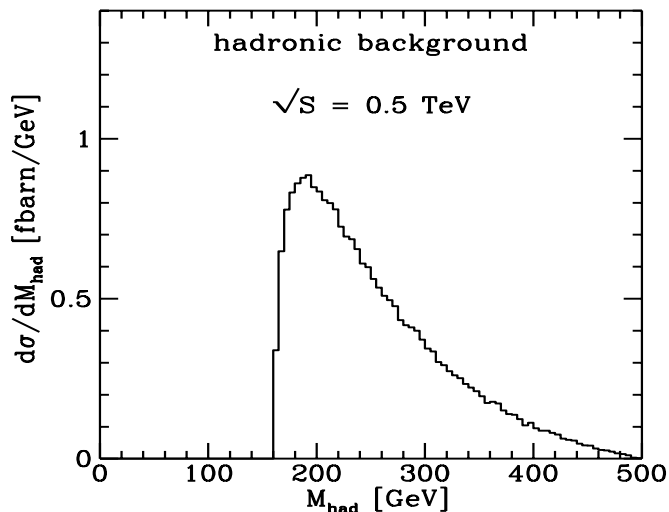


Figure 3: Invariant hadronic mass distribution in the process $e_L^- e_L^- \rightarrow e^- e^- W^- W^+ \rightarrow e^- e^- + jets$ in the Weizsäcker-Williams approximation.

4 Discovery Limits

To summarize, imposing cuts on the invariant hadronic mass, m_{had} , and the average transverse momentum of the jets, $p_\perp(aver.)$, the background to the signal process $e_L^- e_L^- \rightarrow W^- W^- \rightarrow jets$, which is characterized by the two parameters m_N and U_{eN} , can be significantly reduced. As discussed in section I, there are constraints from low energy data. While neutrinoless double beta decay is the most stringent constraint (see eq. (10)) for neutrino masses below 660 GeV, the bound from charged current universality ($U_{eN}^2 < 4 \times 10^{-3}$) dominates for larger masses. As in our plots the mass is mostly larger than 660 GeV we did not plot the bound from $\beta\beta_{0\nu}$. Requiring a signal/background ratio > 1 and the number of signal events to be > 20 , we worked out the discovery limits in the (m_N, U_{eN}^2) -plane. The results for $\sqrt{s} = 500$ GeV are shown in Fig. 6, assuming a luminosity $L = 50 fb^{-1}$ and requiring the average momentum of the jets $p_\perp(aver.)$ to be > 25 GeV. In this figure the horizontal line represents the bound from charged current universality and/or LEP-1 data. Imposing the cut on m_{had} at 450 GeV the allowed region in the parameter space is above the solid curve and below the horizontal line. If m_{had} is cut at 400 GeV the allowed region lies between the dashed curve and the horizontal line. From the figure one sees, that it is very crucial at which value the cut on m_{had} is imposed. Cutting at 400 GeV, the allowed parameter space is essential empty; if the cut is imposed at 450 GeV, one is sensitive to a rather large parameter space: masses up to 2 TeV could be discovered. In an ideal experimental situation, without any fluctuations in \sqrt{s} , one would of course make the m_{had} -cut basically at \sqrt{s} . In the real situation this energy is smeared, however, by beamstrahlung and initial state radiation. Of course one could simulate these effects in order to find out the optimal value at which the m_{had} -cut should be imposed. Also the cut on the average transverse momentum was imposed in a rather arbitrary, but reasonable way; also this cut could be optimized in order to become sensitive to a somewhat larger parameter space.

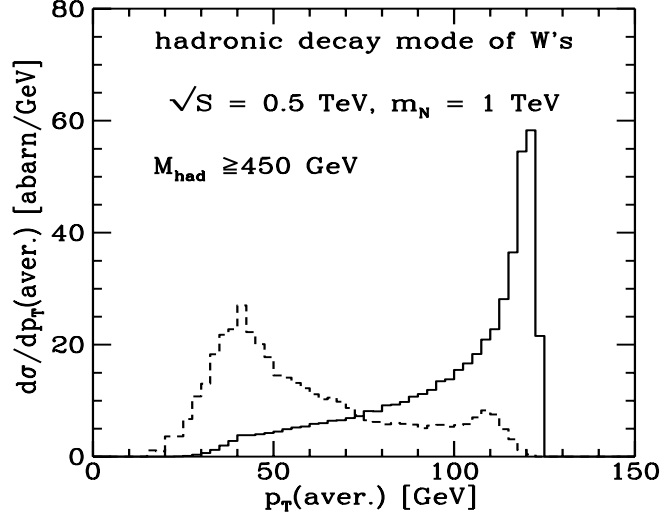


Figure 4: Signal (solid line) and background (dashed line) as a function of the average transverse momentum $p_{\perp}(aver.)$ of the jets. The hadronic invariant mass is required to be $m_{had} \geq 450$ GeV and the other parameters are chosen to be $\sqrt{s} = 500$ GeV, $m_N = 1$ TeV, $U_{eN}^2 = 4 \times 10^{-3}$.

The corresponding results for $\sqrt{s} = 1$ TeV and $L = 100 fb^{-1}$ are shown in Fig. 7. It is impressive that one is sensitive to neutrino masses up to 12 TeV, assuming the mixing angle at its present upper bound.

5 CP violating phase from the interference region

In this section we wish to discuss an alternative scenario [6], [7], with **two** relatively light heavy neutrinos according to

$$m_W \ll \sqrt{s} \lesssim m_{N_1} \leq m_{N_2} \ll m_{N_3}, \dots \quad (14)$$

In this case an interference can arise at the level of the single helicity amplitude $e_L^- e_L^- \rightarrow W_L^- W_L^-$. To make this more explicit, we rewrite the cross section (11) using the parametrization

$$\begin{aligned} m_{N_1} U_{eN_1}^2 &= e^{i\lambda} [a e^{i\delta/2}] \quad ; \quad m_{N_2} U_{eN_2}^2 = e^{i\lambda} [b e^{-i\delta/2}] \\ q_1 &= (m_{N_1})^2 \quad ; \quad q_2 = (m_{N_2})^2 \quad ; \quad q_1 < q_2 \quad , \quad a, b \geq 0 \text{ (real)} \quad . \end{aligned} \quad (15)$$

The differential cross section which does not depend on the overall phase λ , then reads

$$\frac{d\sigma}{d\cos\theta} = \frac{G_F^2}{2\pi} X \quad , \quad (16)$$

with

$$\begin{aligned} X &= |a e^{i\delta/2} f_1 + b e^{-i\delta/2} f_2|^2 \quad \text{or} \\ X &= a^2 f_1^2 + 2abc f_1 f_2 + b^2 f_2^2 \quad , \\ f_i &= \frac{tu - \frac{1}{2}(t+u)q_i}{(t-q_i)(u-q_i)} \quad (i = 1, 2) \quad . \end{aligned} \quad (17)$$

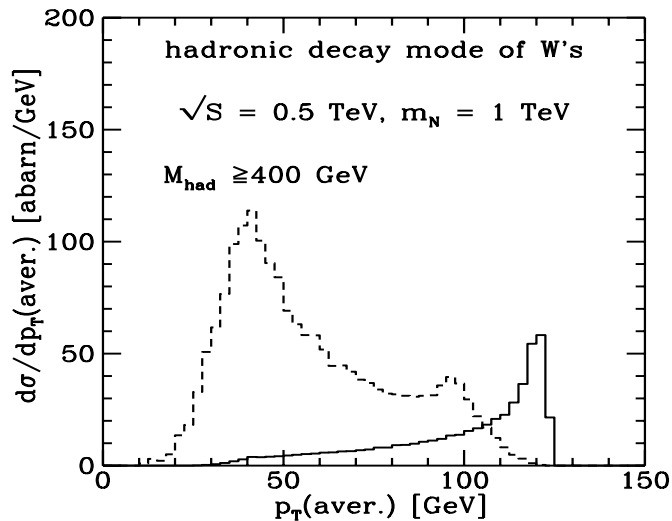


Figure 5: Same as Fig. 4, but for $m_{had} \geq 400$ GeV.

In eq. (17) $c = \cos \delta$ is the cosine of the relative phase between $m_{N_1} U_{eN_1}^2$ and $m_{N_2} U_{eN_2}^2$, while the quantities $t, u, s = t + u$ and $X = X(t, u)$, are understood to be measurable at any suitable finite set of values for the kinematic variables. As seen from eq. (17), the reduced cross section X depends on the 5 real parameters

$$a, b, q_1, q_2 > 0 \quad \text{and} \quad c = \cos \delta \quad ; \quad -1 \leq c \leq 1 \quad (18)$$

The process $e_L^- e_L^- \rightarrow W^- W^-$, in the sense of a leading approximation, does not exhibit direct CP (or T) violation. A nonvanishing CP violation only results, if in addition to the CP odd phase δ also a CP even phase α , generated by the electromagnetic interaction, is involved [7] (e.g. through Coulomb exchange in the initial state). This is in analogy to direct CP violation in weak decays of hadrons: δ plays the role of a CKM angle, while α is to be identified with a phase generated by the strong interaction. In order to find CP violation experimentally, the pair of CP associated reactions $e_L^- e_L^- \rightarrow W^- W^-$ and $e_R^+ e_R^+ \rightarrow W^+ W^+$ needs to be observed with high statistics, an unrealistic endeavour for the two reactions at hand. High statistics and precision are (would be) mandatory because it is the difference of respective differential cross sections which reveals the sought CP asymmetry. This difference, which would be strictly zero neglecting electromagnetic initial- or final state interaction, is much smaller (by a factor α) than the individual interference patterns.

As the interference pattern is much more readily observable - due to its leading character - than any actually CP violating effect, we concentrate on working out a strategy to establish (or refute!) the CP violating angle δ , which enters the differential cross section through its cosine. Assuming the discovery of the reaction $e_L^- e_L^- \rightarrow W^- W^-$ at some initial c.m. energy, predominantly due to the exchange of a single (noninterfering) heavy Majorana neutrino, it is well conceivable that the sought interference can be established when going to higher energies.

From eq. (17) it becomes clear that all the 5 parameters a, b, c, q_1 , and q_2 (within their respective ranges as shown in eq. (18)) can be extracted in principle from suitable data,

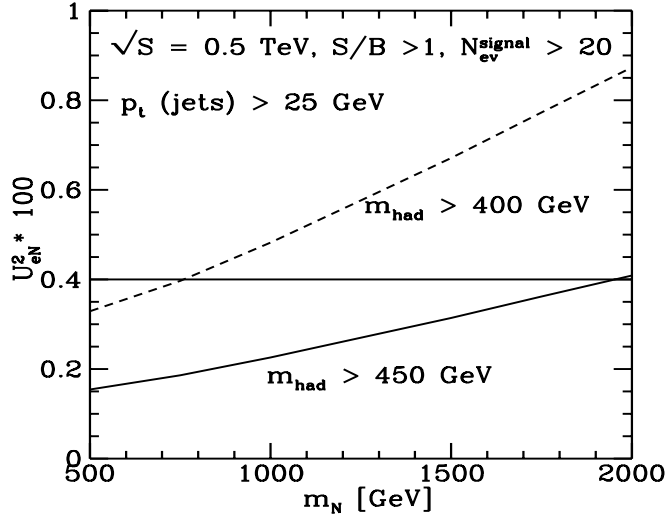


Figure 6: Discovery limits in the (m_N, U_{eN}^2) -plane for $\sqrt{s} = 500$ GeV and luminosity $L = 50 fb^{-1}$. The horizontal solid line at $U_{eN}^2 = 4 \times 10^{-3}$ represents the upper bound on U_{eN}^2 from charged current universality. Requiring $p_{\perp}(aver.) > 25$ GeV and $m_{had} > 450$ GeV, the allowed region in the parameter space is above the solid curve and below the horizontal line. Using the looser cuts $p_{\perp}(aver.) > 25$ GeV and $m_{had} > 400$, the allowed region lies above the dashed curve and below the horizontal line.

assuming this interference scenario is realized in nature with a sufficiently large cross section. To emphasize again, a value for $c = \cos \delta$ different from ± 1 would establish the existence of CP violation.

As this issue might become relevant in future, we decided to elaborate a detailed strategy to extract the values of the parameters from data. However, as the details of this discussion are necessarily technical, we relegate it to the appendix.

6 Summary and Conclusions

In this paper we have investigated what can be learnt about the (heavy) neutrino sector from the reaction $e_L^- e_L^- \rightarrow W^- W^-$ at future colliders. In a first scenario we have assumed that only one of the heavy neutrinos is light enough to lead to a detectable cross section. For this case we have worked out discovery limits in the (m_N, U_{eN}^2) -plane. We found that at the c.m. energy $\sqrt{s} = 500$ GeV neutrinos with masses up to 2 TeV can be discovered, assuming the relevant mixing angle to be at its present bound originating from low-energy experiments. At $\sqrt{s} = 1$ TeV, the discovery region is much larger: Neutrinos with masses up to 12 TeV can be discovered. For the discovery of heavy neutrinos $e^- e^-$ colliders are better suited than $e^+ e^-$ machines, because in the latter case the neutrinos have to be produced; consequently, one is only sensitive to neutrino masses smaller than \sqrt{s} . However, once a heavy neutrino is found, its properties (like decay channels etc.) could be better investigated in an $e^+ e^-$ environment (with sufficient energy). Therefore, as in many other aspects, $e^+ e^-$ and $e^- e^-$ colliders are

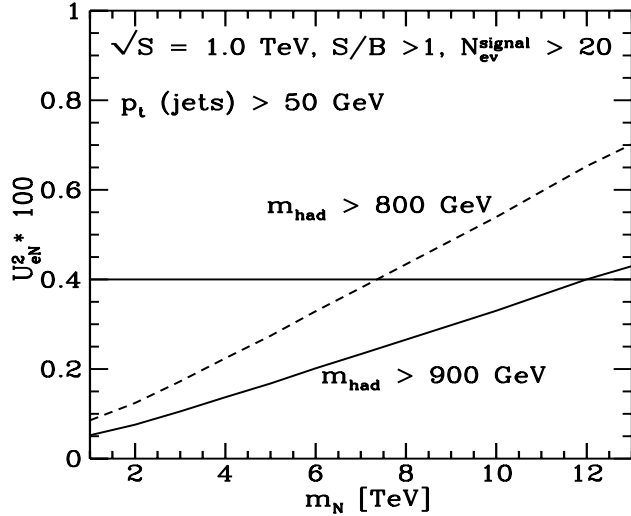


Figure 7: As Fig. 6, but for $\sqrt{s} = 1$ TeV and luminosity $L = 100 fb^{-1}$. The solid line corresponds to $m_{had} > 900$ GeV and $p_{\perp}(aver.) > 50$ GeV, while the dashed line is for $m_{had} > 800$ GeV and $p_{\perp}(aver.) > 50$ GeV. The horizontal line again represents the upper bound on U_{eN}^2 from charged current universality.

complementary.

Finally, we have investigated a scenario where two of the heavy Majorana neutrinos are relatively light. There, in principle the relative phase δ between the mixing parameters can be measured. This phase is responsible for manifest CP violation in $e_L^- e_L^- \rightarrow W^- W^-$: If $\delta \neq 0, \pi$, direct CP violation is established. For this reason we have discussed a rather detailed strategy how to extract this phase from data.

Acknowledgments: We thank F. Cuyper, T. Han and C.A. Heusch for helpful discussions and the organizers of the Snowmass Workshop for a wonderful time in Colorado.

Appendix

A Strategy to extract the CP violating phase

As seen from eq. (17), the reduced cross section X is a rational function in the variables t and u , i.e., of the form $X = g/h$, where g and h are symmetric polynomials in t and u . For the

following it is useful to write this somewhat more explicitly as

$$X = X(t, u) = \frac{g_{\mu\nu} t^\mu u^\nu}{h_{\alpha\beta} t^\alpha u^\beta} \quad , \quad (19)$$

where $g_{\mu\nu} = g_{\nu\mu}$ and $h_{\alpha\beta} = h_{\beta\alpha}$ are the coefficients of the symmetric polynomials g and h , respectively. In eq. (19) the obvious summations are tacitly understood. These coefficients themselves depend on the set of parameters $\underline{\Pi} = [a, b, c, q_1, q_2]$ we finally want to extract, more precisely

$$h_{\alpha\beta} (q_1, q_2) \quad , \quad g_{\mu\nu} (a, b, c ; q_1, q_2) \quad . \quad (20)$$

For mathematical reason, as we will discuss later, it is convenient to extract in a first step the coefficients $g_{\mu\nu}$ and $h_{\alpha\beta}$ without making use of their functional dependence on the parameters. Only after having determined these coefficients we use the functional dependence in order to extract the parameter set $\underline{\Pi}$. This has the most welcome advantage, that the analysis done in this way becomes sensitive to scenarios where one heavy Majorana neutrino interferes with some "other mechanism" (with a dependence of the same form with respect to t and u) which also contributes to the process $e_L^- e_L^- \rightarrow W^- W^-$. As this process violates lepton number conservation, this "other mechanism" necessarily corresponds to new physics different from heavy Majorana neutrino exchange.

A.1 Extraction of the coefficients $g_{\mu\nu}$ and $h_{\alpha\beta}$

From the explicit form of the functions f_i in eq. (17), one easily finds that the indices (=powers of t and u) μ, ν, α, β in eq. (19) range from 0 to 4. In general such symmetric polynomials have 15 independent coefficients. More detailed inspection of the polynomial h shows that the coefficient $h_{44} = 1$, while the remaining coefficients of h depend on the parameters q_1 and q_2 . For the polynomial g the coefficients $g_{00} = 0$, $g_{01} = 0$ (and therefore also $g_{10} = 0$) while the other 13 coefficients depend on the parameters q_1, q_2, a, b , and c . In total there are 14+13=27 nontrivial coefficients. We now put eq. (19) into the form

$$h_{\alpha\beta} [t^\alpha u^\beta X] - g_{\mu\nu} t^\mu u^\nu = 0 \quad . \quad (21)$$

In eq. (21) a linearly factorized form is achieved, separating the nonredundant subset of determinable quantities

$$X_{\alpha\beta} = \frac{1}{2} (t^\alpha u^\beta + t^\beta u^\alpha) X ; T_{\mu\nu} = \frac{1}{2} (t^\mu u^\nu + t^\nu u^\mu) \quad (22)$$

from the set of quantities to be determined (=unknowns)

$$h_{\alpha\beta} \quad , \quad g_{\mu\nu} \quad . \quad (23)$$

Taking into account the constraints on the coefficients $g_{\mu\nu}$ and $h_{\alpha\beta}$ mentioned in the text, eq. (21) takes the inhomogeneous linear form

$$\begin{aligned} X_0 + X_{\alpha\beta} h_{\alpha\beta} + T_{\mu\nu} (-g_{\mu\nu}) &= 0 \quad (\rightarrow \Delta \approx 0) \\ \alpha\beta \neq 44 & ; \quad X_0 = X_{44} = (tu)^4 X \\ \mu\nu \neq 00, 10, 01 & \end{aligned} \quad (24)$$

The expression $0 (\rightarrow \Delta \approx 0)$ in eq. (24) reflects the fact that there are systematic deviations from the hypothetical relation in eq. (24) - theoretical as well as experimental - beyond the statistical errors, where the latter are unproblematic from the mathematical point of view.

We now form the two vectors of unknowns z_ℓ and associated determinables X_0, D_ℓ , restricting ourselves to the nonredundant set as specified in eq. (24)

$$\begin{aligned} \{z_\ell\} &= \{h_{\alpha\beta}; -g_{\mu\nu}\} \quad ; \quad \{D_\ell\} = \{X_{\alpha\beta}; T_{\mu\nu}\} \\ \{\ell = 1, \dots, 14\} &\leftrightarrow \{0 \leq \alpha \leq \beta \leq 4; \alpha\beta \neq 44\} \\ \{\ell = 15, \dots, 27\} &\leftrightarrow \{0 \leq \mu \leq \nu \leq 4; \mu\nu \neq 00, 01\} \end{aligned} \quad (25)$$

The association $D_\ell \leftrightarrow \{X_{\alpha\beta}; T_{\mu\nu}\}$ for $\alpha \neq \beta$ or $\mu \neq \nu$ is

$$D_\ell = \begin{cases} 2X_{\alpha\beta} & \text{for } \alpha < \beta \leftrightarrow \ell = 1, \dots, 14 \\ 2T_{\mu\nu} & \text{for } \mu < \nu \leftrightarrow \ell = 15, \dots, 27 \end{cases} \quad (26)$$

in order to take into account the symmetric summation relative to the indices $\alpha \neq \beta$ and $\mu \neq \nu$. Then eq. (24) is cast into conventional linear form

$$\begin{aligned} X_0 + \sum_{\ell=1}^{27} D_\ell z_\ell &= 0 (\rightarrow \Delta \approx 0) \\ \{X_0, D_\ell, \Delta, \} &= \{X_0, D_\ell, \Delta, \} (t, u) \end{aligned} \quad (27)$$

In eq. (27) $\{X_0, D_\ell\}$ are measured or exactly known functions, while Δ is an unknown function of the kinematic variables. The latter is set 0 whenever possible, but should be kept in the equation in order to avoid eventual inconsistencies, which typically arise when the signal (or the full details of the assumed interference pattern) are insignificant relative to the systematically misinterpreted background, systematic and/or statistical measurement errors.

To the nonredundant ℓ set, consisting of the functions and unknowns $\{D_\ell, z_\ell, X_0; \Delta\}$ we associate - one by one - a given $\{k\}$ set ($k = 1, \dots, 27$) in the following way: we **choose** a set of weight functions over the region of experimentally accessible kinematic variables t, u

$$\begin{aligned} \{w_k\} &: w_k = w_k(t, u); \quad k = 1, \dots, 27 \\ X_0 &\rightarrow (X_0)_k = \int dt du w_k X_0 \\ D_\ell &\rightarrow D_{k\ell} = \int dt du w_k D_\ell \\ \Delta &\rightarrow \Delta_k = \int dt du w_k \Delta \end{aligned} \quad (28)$$

The weighting functions w include delta functions singling out

- individual points or idealized bins $(t, u)_k$.
- line integrals, e.g. angular integrals with fixed c.m. energy.

There exists an infinite number of different $\{k\}$ sets, each one defined through a given choice of 27 weighting functions $\{w_k\}$; ($k = 1, \dots, 27$).

We concentrate on a given set to be interpreted as sample case. Eq. (27) is thus transformed to an inhomogeneous linear system of equations

$$X_0 + D z = 0 \ (\rightarrow \Delta \approx 0) \quad , \quad (29)$$

where we use matrix notation in order to suppress component indices.

In the present context the standard notions of linear algebra receive specific interpretations. The regular case applies to a nonvanishing determinant of D . Because of the approximate nature of eq. (29), a vanishing and approximately vanishing determinant are equivalent in a sense to be precisely defined. The irregular case corresponds necessarily to the situation where the data **does not allow** to derive the hypothetical interference pattern, i.e. where the sought parameter $c = \cos \delta$ cannot be significantly determined. While also this case constitutes useful information, we concentrate now on the more interesting regular case.

In order to generate at least one $\{k\}$ set, at least 27 bins are needed. We choose one more in order to enable error analysis. This presupposes that at least of order 140 to 240 events fall into these 28 bins. As an example we may choose the 28 bins by taking 4 fixed c.m. energies and 7 angular bins for each; the actual choice, however, is irrelevant for the following. One then can form maximally 28 $\{k\}$ sets leaving out one of the 28 bins in turn. We number each $\{k\}$ set with the index $\{n\}$ ranging from 1 to 28.

Thus 28 matrices $D^{\{n\}}$ result, which we individually subject to predetermined criteria³ for qualifying as a regular matrix. These criteria will translate into lower bounds for the determinants depending on $D^{\{n\}}$

$$\left| \text{Det } D^{\{n\}} \right| > C(\{n\}) > 0 \quad . \quad (30)$$

In general not all matrices $D^{\{n\}}$ will pass the test in eq. (30). Thus the last condition defining the regular case is to specify the fraction of $\{k\}$ sets for which the test in eq. (30) is successful. To fix ideas we set this fraction to 75 %.

Having finally defined the regular case, we assume in the following that the data qualifies as regular. We retain only those $\{k\}$ sets, which pass the test in eq. (30). We (re)number them with the label $\{n_+\}$

$$n_+ = 1, \dots, N_+ \ ; \ 21 \leq N_+ \leq 28 \quad . \quad (31)$$

The range for N_+ , the number of regular $\{k\}$ sets, corresponds to the 75 % limit required above. We compare the calculational effort required to establish the regular case with a direct χ^2 minimalization procedure to determine the five parameters at hand. Following the present method the extraction of $28 \times 27 \times 27 + 28 = 20'400$ quantities $X_{0,n}, D^{\{n\}}$ was required. This corresponds to between 7 and 8 values for each of the five parameters ($7.3^5 \approx 20'400$).

Now we determine the unknowns z from eq. (29) setting the systematic deviation vector $\Delta = 0$ for each retained $\{k\}$ set

$$(z = -D^{-1} X_0)_{\{n_+\}} \ ; \ n_+ = 1, \dots, N_+ \quad . \quad (32)$$

We can assign weights to each regular $\{k\}$ set, in inverse proportion to the estimated quadratic standard deviation

$$p_n \ ; \ \sum p_n = 1 \quad . \quad (33)$$

³We do not discuss here details of these criteria, straightforward to define, which are to be used to eliminate the irregular case.

In eq. (33) and in the following the index + for $n_+ = 1, \dots, N_+$ is omitted. We then form the mean value and relative error correlation matrix

$$\bar{z} = \sum p_n z_{\{n\}}; \varrho_{\ell\ell'}^2 = \sum p_n \frac{(z_{\{n\}} - \bar{z})_\ell (z_{\{n\}} - \bar{z})_{\ell'}}{\bar{z}_\ell \bar{z}_{\ell'}} \quad (34)$$

The estimate of the error matrix $\varrho_{\ell\ell'}^2$ in eq. (34) is only sufficient to estimate the correlation matrix for $N_+ - 1$ out of the $N = 27$ components z_ℓ . Nevertheless we can perform a χ^2 minimization - not to be confused with a statistical χ^2 - on the systematic deviations Δ_n in eq. (29), which we have set to zero in the first approximation step displayed in eq. (32). To this end we cast the set of eqs. (32) into the form

$$\begin{aligned} D^{\{n\}} (z - z_{\{n\}}) &= \Delta_{\{n\}}; z_{\{n\}} = - (D^{\{n\}})^{-1} X_0^{\{n\}} \\ \chi^2 &= \sum p_n \Delta_{\{n\}}^2 \end{aligned} \quad (35)$$

In eq. (35) we have used the euclidean norm $\Delta_{\{n\}}^2 = \sum_k (\Delta_{\{n\}})_k^2$ to evaluate the systematic deviation of $\Delta_{\{n\}}$ from 0.

We determine the minimum and standard deviation of the function $\chi^2(z)$ defined in eq. (35)

$$\begin{aligned} \chi^2 - \chi_{min}^2 &= (z - \langle z \rangle)^T \langle D^2 \rangle (z - \langle z \rangle) \\ \chi_{min}^2 &= \sum p_n \left[D^{\{n\}} (\langle z \rangle - z_{\{n\}}) \right]^2 \\ \langle z \rangle &= \langle D^2 \rangle^{-1} \sum p_n D^{\{n\} T} D^{\{n\}} z_{\{n\}} \\ \langle D^2 \rangle &= \sum p_n D^{\{n\} T} D^{\{n\}} \end{aligned} \quad (36)$$

In eq. (36) the symbol T denotes transposition.

All quantities except the free variable z are functions of the determinables $X_0^{\{n\}}$, $D^{\{n\}}$, depending in a highly nonlinear way on the matrix elements of D . The regular case ensures that the (symmetric) matrix $\langle D^2 \rangle$ is regular.

The χ^2 procedure outlined here is equivalent to a direct fit of the parameters obtained from the hypothesis in the form of eq. (17), using the quadratic deviation function

$$\chi^2 = \left(X - |a e^{i\delta/2} f_1 + b e^{-i\delta/2} f_2|^2 \right)^2 \quad (37)$$

with one notable difference : the relation in eq. (36), quadratic in the free variable z , is functionally exact. In the latter, hypothesis and the determination of determinables are fully separated. The functional dependence of the quantities

$$\left\{ \chi_{min}^2, \langle z \rangle, \langle D^2 \rangle, z_{\{n'\}} \right\} \left[X_0, D^{\{n\}} \right] \quad (38)$$

on the arguments $X_0, D^{\{n\}}$ and p_n is known and exact. The first two arguments, defined in eqs. (22) - (28), involve, beyond the cross section, known auxiliary functions used to formulate the hypothesis but as such are independent of it. Their determination is subject to systematic and statistical **measurement errors only**. These can be analyzed independently to any test of the hypothesis.

Furthermore all errors, including the incomplete theoretical knowledge of signal as well as remaining background amplitudes, are fully accounted for by the unknown quantities $\Delta_{\{n\}}$ defining the function χ^2 according to eq. (35).

σ contours

The regular case ensures a pronounced minimum of $\Delta\chi^2(z)$ at $z = \langle z \rangle$. This is not surprising, since the conditions in eq. (30) defining the regular case qualify the hypothesis as viable (necessary but not sufficient conditions).

We consider the $(f - \sigma)$ contours ($f = 1, 2, \dots$) bounding the regions of z values

$$\Delta\chi^2(z) = (z - \langle z \rangle)^T \langle D^2 \rangle (z - \langle z \rangle) \leq f^2 \chi_{min}^2 \quad (39)$$

The probabilistic syntax inherent to the notion of σ contour is only true under the following circumstances

- a) all systematic deviations are zero and the hypothesis is true.
- b) the systematic deviations $\Delta_{\{n\}}$ are themselves independent stochastic variables and the hypothesis is true.

Case a) above applies in an approximative sense to the situation where statistical errors dominate. This will most probably be the case, whenever the lepton violating signals discussed here will become observable for the first time.

Nevertheless the value of f to be applied to the following analysis is a matter of initially judicious choice to be followed by subsequent checks. The method at hand allows several such checks with the same data. The first consists in comparing the value for $\langle z \rangle$ with \bar{z} defined in eq. (34)

$$\Delta\chi^2(\bar{z}) = \bar{f}^2 \chi_{min}^2 \quad (40)$$

Irrelevant systematic deviations imply the relations involving \bar{f} in eq. (40)

$$\bar{f} \approx 1 ; \bar{f}^2 \chi_{min}^2 = O \left(\bar{z}^T \varrho^2 \bar{z} \parallel \langle D^2 \rangle \parallel \right) \quad (41)$$

In eq. (41) ϱ^2 denotes the variance matrix estimated in eq. (34) and $\parallel \langle D^2 \rangle \parallel$ an appropriate norm, e.g $\parallel \langle D^2 \rangle \parallel = \frac{1}{N} tr \langle D^2 \rangle$.

The tests outlined above can be extended, using the same data, choosing new bins, thus enlarging the number of regular $\{k\}$ sets. It is understood that throughout

$$(\langle z \rangle - z_{\{n\}})^2, (\bar{z} - z_{\{n\}})^2 \ll \langle z \rangle^2, \bar{z}^2 \quad (42)$$

holds. If no satisfactory factor $f = O(1)$ can be found, this means that the hypothesis cannot be significantly established, without separate understanding of systematic deviations.

We continue the discussion on the contrary assumptions, i.e. that a satisfactory $(f - \sigma)$ contour is determined with $f \approx 1$ such that

$$\Delta\chi^2(z_{true}) \leq f^2 \chi_{min}^2 \rightarrow z_{true} \approx \langle z \rangle \quad (43)$$

A.2 Establishing the interference scenario

All disqualifying criteria being positively met, still does not prove the hypothesis of the interference scenario defined in eqs. (14) - (17), because so far we have only determined successfully the vector z , which is nothing but the coefficients $g_{\mu\nu}$ and $h_{\alpha\beta}$ in eqs. (20) and (23) [see also eq. (25)]. The vector z depends on the set of parameters $\underline{\Pi} = [q_1, q_2, a, b, c]$, in which we are ultimately interested in. For each point in the parameter set $\underline{\Pi}$ we calculate $z = z(\underline{\Pi})$. The so determined vectors z sweep out a 5 dimensional subspace, denoted by S_5 , when varying the five parameters $\underline{\Pi}$ in the allowed range specified in eq. (18).

The $(f - \sigma)$ allowed region in the parameter space $\underline{\Pi}$ is the intersection of S_5 with the z region bounded by the corresponding contour according to eq. (39)

$$\{ f - \sigma [\underline{\Pi}] \} = \{ \underline{\Pi} \mid \Delta\chi^2 (z [\underline{\Pi}]) \leq f^2 \chi_{min}^2 \} \quad (44)$$

The final test of our hypothesis of an interference scenario of two heavy neutrino flavors, requires the region of allowed parameters $(f - \sigma [\underline{\Pi}])$ not to be empty or concentrated very near to the bounding $(f - \sigma)$ contour. The best values for the five parameters $[\underline{\Pi}]$ are then determined by the minimum of the function $\Delta\chi^2 (z [\underline{\Pi}])$ in eq. (44)

$$\Delta\chi^2 (z [\underline{\Pi}_{best}]) = \text{Min}_{[\underline{\Pi}]} \Delta\chi^2 (z [\underline{\Pi}]) < f^2 \chi_{min}^2 \quad (45)$$

Amusingly, an interesting situation also arises if this test fails, whereby the specific hypothesis (i.e., the interference of 2 Majorana neutrinos) is definitely disproved. However, on the level of polynomials of the same degree as those defining the hypothesis, an alternative interference pattern is established by the consistent form of the $(f - \sigma)$ contour defined in eq. (43). This positively would prove the interference of the one flavor signal, considered as established according to the criteria discussed in the previous sections, albeit with an amplitude of another nature than the one considered, also violating lepton number! Interference with a standard model background amplitude is by definition excluded.

We continue the discussion for the alternative case where the criteria in eqs. (44) and (45) are satisfied. The full amplitude for two interfering Majorana neutrinos can be reconstructed for all values of the parameters

$$\begin{aligned} q_1 &= (m_{N_1})^2 ; \quad q_2 = (m_{N_2})^2 ; \quad q_1 < q_2 , \quad a, b \geq 0 \\ c &; \quad -1 \leq c \leq 1 \end{aligned} \quad (46)$$

in the allowed region $\{ f - \sigma [\underline{\Pi}] \}$.

On this basis additional tests of the consistency of parametrization with the data can be performed. Furthermore the absolute values of the mixing parameters $| U_{eN_1} |$ and $| U_{eN_2} |$ in eq. (15) can be determined. These are subject to the constraints unrelated to the data sample considered here [5]

$$| U_{eN_1} |^2 + | U_{eN_2} |^2 \leq 4 \times 10^{-4} \quad , \quad (47)$$

eventually narrowing down the acceptable parameter region.

Finally we turn to the most subtle of the five parameters, c , the cosine of the relative phase between $m_{N_1} U_{eN_1}^2$ and $m_{N_2} U_{eN_2}^2$. The significant determination of c relies on a solid error

analysis with respect to the other 4 parameters, since the error matrix must show a high degree of correlation between the errors of c and those of the other parameters. In the vein of the present discussion we assume all further tests to reveal no inconsistencies. Then we foresee the result

$$-1 \leq c_- \leq c_{best} \leq c_+ \leq 1 \quad (48)$$

according to the $(f - \sigma)$ criteria defined in eqs. (43) , (44) and (45).

Three distinct possibilities arise, in ascending order of interest:

- 1) c_+ is not significantly different - within $(2 - \sigma)$ say - from 1, **nor** is c_- from -1.
- 2) **either** c_+ is not significantly different from 1, **or** c_- insignificantly from -1.
- 3) c_+ **is** significantly different from 1, **and** c_- from -1.

Case 1) is unlikely, given the severe criteria in particular those regarding the regular case, discussed above, but cannot be entirely excluded. The conclusion is that the interference pattern can be established for some part of the allowed parameter region but the error margin is too large for an actual determination of c .

Case 2) establishes the interference pattern but does not exclude the CP conserving relative phases $\delta = 0, \pi$.

Finally case 3), which serves as motivation of this analysis, not only establishes - within the errors - the interference pattern but proves, albeit indirectly, the CP violating character of this interference.

We shall conclude this discussion on the hypothesis that this last case prevails.

References

- [1] W. Buchmüller and C. Greub, *Nucl. Phys.* **B363** (1991) 345;
W. Buchmüller et al., in: Proceedings of the Workshop "e⁺e⁻ collisions at 500 GeV: the Physics Potential", Part B, DESY 92-123B, August 1992, p. 539.
- [2] T. Yanagida, in Workshop on Unified Theories, KEK report 79-18, (1979) p. 65;
M. Gell-Mann et al., in Supergravity, eds. P. van Nieuwenhuizen and D. Freedman (North-Holland, Amsterdam, 1979) p. 315.
- [3] A. Djouadi, J. Ng and T. G. Rizzo, SLAC-PUB-6772, hep-ph/9504210 in: Electroweak Symmetry Breaking and Beyond the Standard Model, edited by T. Barklov, S. Dawson, H.E. Haber and S. Siegrist, World Scientific. *Phys. Rev.* **D50** (1994) 6704.
- [4] C. A. Heusch and P. Minkowski, preprint SCIPP 96/41, BUTP 96/25 [hep-ph/9611353].
- [5] C.A. Heusch and P. Minkowski, *Nucl. Phys.* **B416** (1994) 3;
J. Gluza and M. Zralek, *Phys. Lett.* **B362** (1995) 148;
G. Bélanger, F. Boudjema, D. London and H. Nadeau, *Phys. Rev.* **D53** (1996) 6292.
- [6] P. Minkowski, *Int. J. Mod. Physics A* **11** (1996) 1591.
- [7] B. Ananthanarayan and P. Minkowski, *Phys. Lett.* **373B** (1996) 130.

- [8] F. Cuyppers, K. Kolodziej and R. Rückl, *Nucl. Phys.* **B430** (1994) 231.
- [9] V. Barger, J.F. Beacom, K. Cheung and T. Han, *Phys. Rev.* **D50** (1994) 6704.
- [10] P. Minkowski, "Aspects of scalar production ($m_h \leq 300$ GeV) in the e^-e^- collider operating mode", in these proceedings.
- [11] Our Montecarlo is based on routines developed by: A. Ali, B. v. Eijk and I. ten Have, *Nucl. Phys.* **B292** (1987) 1.